MIAN-013
12/12

Interface structure and Schottky barrier height of buried $CoSi_2$/Si(001) layers

P. Werner[a] and W. Jäger
Institut für Festkörperforschung, Forschungszentrum Jülich, D-52425 Jülich, Germany

A. Schüppen
Institut für Schicht- und Ionentechnik, Forschungszentrum Jülich, D-52425 Jülich, Germany

(Received 7 October 1991; accepted for publication 2 June 1993)

The atomic interface structure of implanted buried layers in (100) oriented Si substrates has been characterized by quantitative high-resolution transmission electron microscopy on cross-section specimens. The buried layers were produced by high-dose Co^+ ion implantation [100 and 200 keV Co^+ ions, $(1–2)\times10^{17}$ cm^{-2}] at 350 °C and subsequent rapid thermal annealing at 750 and at 1150 °C. Planar interface regions of high perfection with domains of different atomic interface structures, and interface steps, frequently with {111} facets, were observed. Comparison with computer-simulated images for various interface models yields evidence for interface regions with six-fold and eight-fold coordination of the Co interface atoms. Furthermore, regions with interfaces showing a continuous transition as well as Co-rich interfaces were found. Measurements of the Schottky barrier heights have been performed and show smaller values for the upper $CoSi_2$/*n*-Si(001) interfaces than for the lower ones. Possible correlations between the interface structures and the resulting electronic properties are discussed.

I. INTRODUCTION

High-dose implantation of Co^+ ions at medium energies and temperatures into Si substrates followed by subsequent annealing allows the production of continuous buried $CoSi_2$ layers.[1–4] This technique, generally referred to as "mesotaxy",[1] can be used to fabricate synthetic structures that utilize the favorable properties of these metallic silicide layers, such as their stability to high-temperature anneals, their low specific electrical resistivity of typically about 15 $\mu\Omega$ cm, and their perfect epitaxial growth because of a crystal structure with a lattice mismatch with Si of only −1.2%. Such epitaxial silicides are of growing interest because of applications in electronic solid-state devices such as metal-base[5] or permeable-base transistors,[6,17] and as contact or interconnect material.[7]

In (001) Si substrates the interfaces of buried $CoSi_2$ layers are generally faceted, in contrast to atomically smooth interfaces of silicide layers found in (111) Si substrates. Such {111} interfaces are energetically favored.[8] Interface models, initially proposed for the atomic structure of $NiSi_2$/Si(001) interfaces, consider two possible atomic structures with six-fold and eight-fold coordinated metal atoms in the interface.[9] The existence of such interface structures could be identified in high-resolution transmission electron microscopy (HRTEM) studies of $NiSi_2$/Si(001) interfaces[9] and of $CoSi_2$/Si(001) interfaces.[10] Recently, a (2×1) reconstruction of Si dimers was proposed as a stable structure of $CoSi_2$/Si(001) interfaces grown by molecular beam epitaxy.[11] A Si-rich interface structure with dimer configuration was proposed from extended HRTEM investigations of ion-implanted $CoSi_2$ layers.[12] A different interface reconstruction was found using *Z*-contrast imaging in scanning transmission electron microscopy.[13]

In view of possible technical applications in fast transistors it is of particular interest to have a detailed knowledge of the correlation of the atomic interface structure with electronic properties. The interface structure should have a decisive influence on the electrical properties, such as barrier heights (SBH) of $CoSi_2$/Si(001) Schottky diodes. According to theoretical considerations about Schottky barrier heights the position of the Fermi level at the interface is influenced by different structure parameters, such as work functions, electron affinity, and charge densities in the interface regions. Crystal defects in the interface are considered in the concept of Fermi-level pinning. It could be shown experimentally that the SBH is influenced by interface orientations. For a $NiSi_2$/*n*-Si(001) a SBH of 0.4 eV was measured, whereas for a $NiSi_2$/*n*-Si(111) *B* interface 0.79 eV was determined.[14] For Si(111) differences of the SBH also occur for twinned *B* and nontwinned *A* crystal transitions and *A*/*A*/*A* heterostructures, respectively.[15] Such large SBH differences for the same material combination cannot be explained by a Fermi-level pinning mechanism. The atomic structure of the interface itself, i.e., coordination of metal atoms and point defects in the interface, is expected to strongly influence the SBH.[14]

In this paper we describe a HRTEM study of the atomic structure of the $CoSi_2$/Si(001) interfaces of continuous buried layers formed by high-dose implantation and subsequent rapid thermal annealing. The experimental results are discussed in the context of the formation of such layers and of the possible influence of different interface structures on the Schottky barrier heights.

[a]On leave from Max-Planck-Institut für Mikrostrukturphysik, D-06120 Halle/Saale, Germany.

 0021-8979/93/74(6)/3846/9/$6.00

II. EXPERIMENTAL

The buried $CoSi_2$ layers have been produced by 100 and 200 keV Co^+ implantation into Si(001) substrates at 350 °C with doses of $(1–2)\times10^{17}$ cm^{-2} followed by subsequent annealing at 750 °C for 30 s and at 1150 °C for 10 s using rapid thermal annealing (RTA) in high-purity argon. Before annealing, the implanted substrates were capped with 200-nm-thick SiO_2 layers. This procedure resulted in interconnected $CoSi_2$ layers with a typical thickness of about 80 nm at a distance of 90 nm below the substrate surface for the higher implantation energy used (Fig. 4), in good agreement with Rutherford backscattering analysis.[16]

Cross-section specimens for HRTEM were prepared by mechanical dimpling and Ar^+ ion milling at 5 keV on a liquid-nitrogen-cooled specimen stage. The final polishing was carried out at a lower ion energy to minimize surface damage.

The HRTEM observations were made in a JEOL-4000EX operated at 400 kV (spherical aberration coefficient $C_s=1$ mm), using the ⟨110⟩ zone axis of thin specimen sections (thickness $t<15$ nm). Conventional bright-field diffraction contrast TEM was applied to characterize defects and the interface roughness over larger interface areas. Imaging conditions were selected to facilitate interpretation of the many-beam lattice image contrast. This relates to the exact alignment of the specimen as well as the electron beam with respect to the optical axis and appropriate defocus values.[10] In our study analyses of the image details included the determination of the {002} lattice plane distance across the interfaces, the shift of the {111} planes inclined to the (001) interface, as well as the geometrical arrangement and intensity of contrast details, as discussed in more detail in the following section. The accurate determination of defocus values in a through-focus series is aggravated by variations of the accelerating voltage and by mechanical vibrations during the exposure of photographic plates. To overcome this problem computer-controlled trough-focus series have been taken using a slow-scan CCD camera (see, e.g., Fig. 7). For the determination of the objective lens defocus during imaging of the wedge-shaped electron microscopy specimens used the analysis of Fresnel fringes at the interfaces turned out to be more accurate than an analysis of amorphous edge regions near the interfaces.

Concerning the fabrication of Schottky mesa diodes a detailed description of the diode technology can be found in Refs. 6 and 17. The Schottky barrier heights of the upper and lower interfaces were determined by *I-V*, *C-V*, and *I-T* measurements for samples which were prepared using the same implantation and annealing conditions as applied for the HRTEM samples. Details of the *I-T* and *C-V* measurements are given in a separate paper.[18]

III. IMAGE SIMULATIONS OF INTERFACE STRUCTURES

For the correct interpretation of HRTEM image details on an atomic scale a quantitative comparison with simulated many-beam images for the corresponding specimen and imaging parameters is required. Such numerical image simulations were performed using the multislice algorithm of the EMS software package.[19] Three different models for the atomic $CoSi_2$/Si(001) interface structure are discussed in the following, which are characterized by different binding configurations of the Si and Co atoms in the interface (Fig. 1).

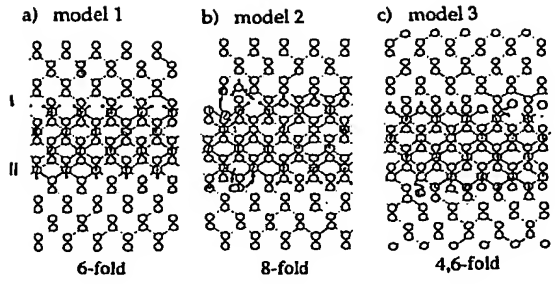

FIG. 1. Crystallographic models of $CoSi_2$/Si(001) interfaces in ⟨110⟩ projection. The silicide lamellae with the two possible interface orientation variants are embedded into the Si matrix; its upper interfaces have configuration I ([110] viewing direction), its lower interfaces have configuration II ([1$\bar{1}$0] viewing direction). (a) Model 1: six-fold coordinated Co interface atoms (Si atoms dark, Co atoms bright). (b) Model 2: eight-fold coordinated Co atoms, Si-rich interface. (c) Model 3: Co-rich interface. Bond lengths and angles between interface atoms are preserved.

The first structural model of the (001) interface is based on the idea of preserving symmetry elements of both crystal lattices, such as mirror axes and mirror glide planes, and was already proposed for the $NiSi_2$/Si(001) interface.[9] In this case the Co atoms at the interface are sitting on a former Si atom position and are six-fold coordinated [Fig. 1(a)]. Experimental observations are performed in two ⟨110⟩ crystal orientations (or projections): in [110] projection the Co atom at the interface sits in {001} direction below a Si atom of the Si lattice (configuration I); in the perpendicular [1$\bar{1}$0] projection the Co atom is shifted by $a/4\langle111\rangle$ (a=lattice constant of Si) from a Si lattice site (configuration II). Dangling bonds of the Co atoms can be saturated by additional Si atoms resulting in the interface model 2, in which the Co atoms are eight-fold coordinated. The corresponding ⟨110⟩ projections of these two models are shown in Figs. 1(a) and 1(b) for a $CoSi_2$ lamella embedded in the Si matrix, with the upper interface representing configuration I ([110]) and the lower interface representing configuration II ([1$\bar{1}$0]). In comparison to model 1 structure model 2 is characterized by a Si-rich interface. A third model considered in the interpretation of the interface images is that of a Co-rich interface which contains an additional layer of ionically bonded Co atoms [model 3, Fig. 1(c)]. These Co atoms are bonded to the Co atoms in the silicide and shifted by $a/4\langle111\rangle$. This interface structure is proposed because it can explain best the image contrast behavior of interface regions close to interface terraces and steps (Sec. IV).

Computer-based image simulations using these models were carried out for ⟨110⟩ lattice projections to establish conditions for the crystal thickness t and the defocus of the

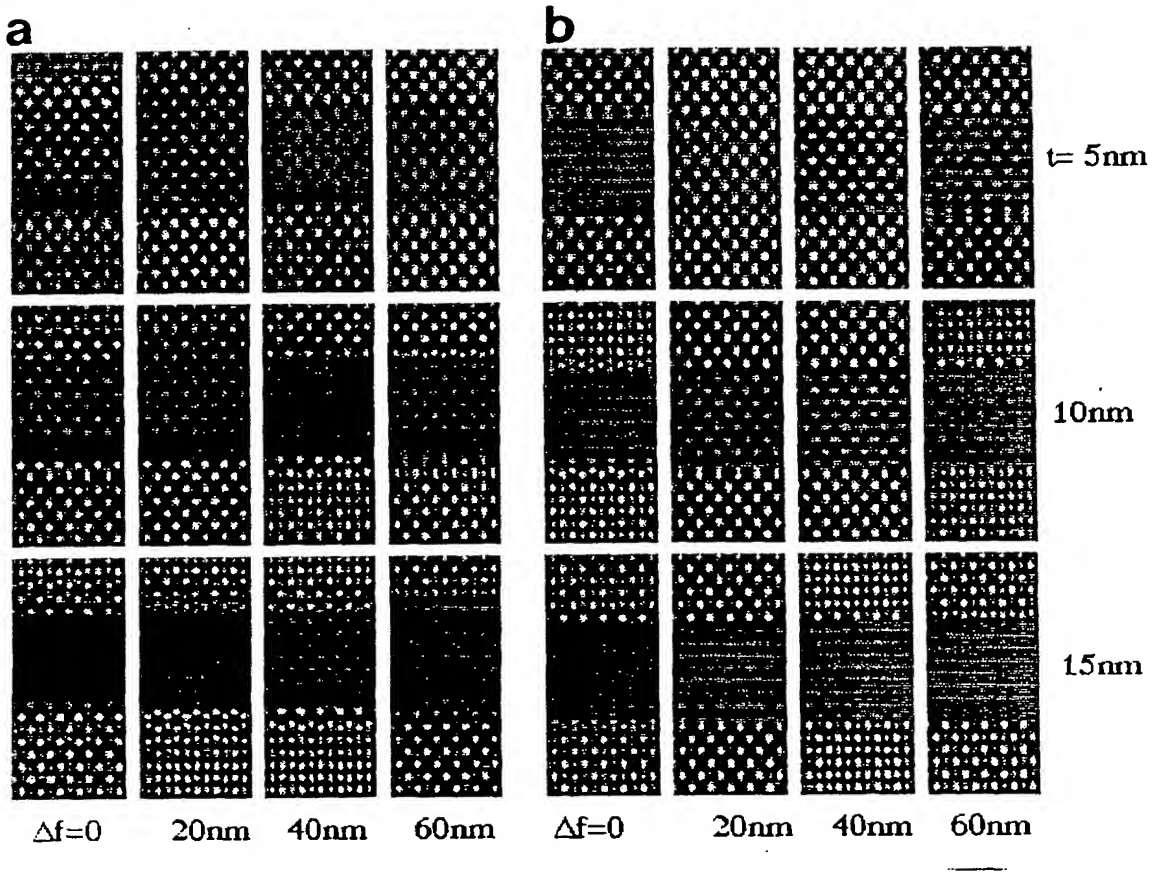

FIG. 2. Computer simulations of the image contrast as a function of the specimen thickness t and the defocus value of the objective lens, Δf, for $CoSi_2$/Si(001) interfaces of structure 1(a) and of structure 2(b) in ⟨110⟩ projection. The images are calculated for a $CoSi_2$ lamella embedded in the Si matrix with the two interface projections I ([110], upper interface) and II ([1$\bar{1}$0], lower interface), according to Fig. 1. Positive Δf values denote underfocus.

objective lens, Δf. This search concerned the influence on image contrast of the amplitude and phase of the {002} wave fields, which are different for $CoSi_2$ compared to Si, and Fresnel diffraction contributions at large defocus values due to the difference of the inner potentials. Examples for such defocus—thickness series of image calculations for the experimentally relevant range of parameters (t,Δf)—are shown in Figs. 2(a) and 2(b) for model 1 and model 2, respectively, and in Fig. 3 for model 3, configuration II. The major results of the image simulations, which are of importance for interpretation of the experimental images of the $CoSi_2$/Si interfaces, can be summarized as follows:

(i) In the range of 20 nm overfocus and 50 nm underfocus the lattice structure of the interface is clearly visible without stronger disturbances by Fresnel diffraction.

(ii) Near the $CoSi_2$/Si(001) interfaces pronounced shifts in the {111} and {200} lattice plane fringes are observed that are characteristic of the different interface structures. A similar behavior has also been described for $NiSi_2$/Si(111),[20–22] for $CoSi_2$/Si(111),[23–25] and for $CoSi_2$/Si(001).[10,12] The accuracy of measurements of rigid shifts across interfaces is 0.03 nm.

(iii) For all three interface structures [Figs. 1(a)–

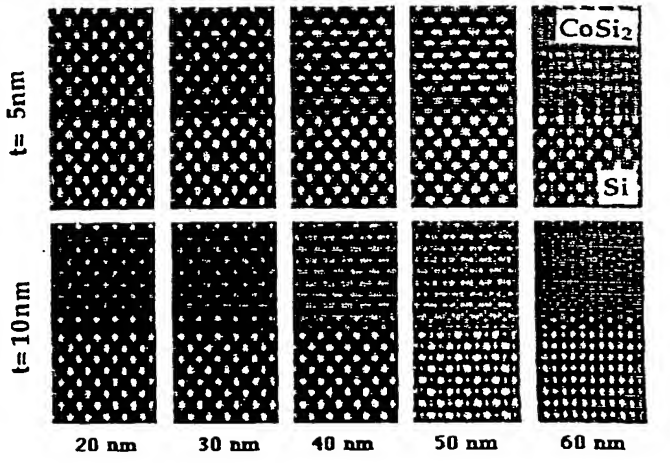

FIG. 3. Computer simulations of the image contrast of $CoSi_2$/Si(001) interfaces of model 3 [Fig. 1(c)] in ⟨110⟩ projection as function of the specimen thickness t and the defocus value Δf. Positive Δf values denote underfocus.

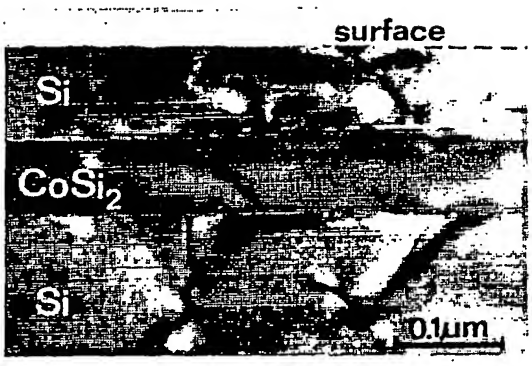

FIG. 4. Cross-section TEM bright-field image of a buried $CoSi_2$ layer of about 80 nm thickness in Si(001) formed after 200 keV Co^+ implantation. The upper interface depicts steps with {111} facets. Dislocations formed by ion implantation and thermal annealing are visible in the Si substrate. Electron beam parallel to interfaces and ⟨110⟩ lattice direction.

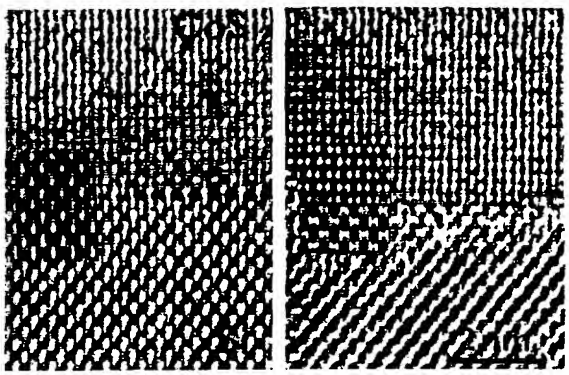

FIG. 5. Comparison between experimental and simulated (inset) images of a model 1 interface (configuration I) at a defocus value of 16 nm (left) and of 48 nm (right). For imaging an objective aperture has been chosen which includes reflections up to {004} and provides a low damping of the envelope of the contrast transfer function.

1(c)] configuration I is characterized by a Z-shaped shift of the {111} planes, whereas in the case of configuration II an opposite (S-shaped) shift of these planes is observed. The {002} lattice plane distance of 0.27 nm is changed at the interface. For model 1 and 2 it amounts to 0.34 nm for orientation relation I and to 0.20 nm for the orientation relation II, respectively. The shifts of the {111} planes across the interfaces amount to ± 0.04 nm ($1/8 d_{\{111\}}$) for these crystallographic models. For the case of the interface structure represented by Fig. 1(c) the shift of the {111} planes amounts to ± 0.12 nm ($\{3/8 d_{\{111\}}\}$), and the distances of the {002} lattice planes are increased by 0.14 nm in comparison to the corresponding distances of configuration I and configuration II of models 1 and 2, respectively.

(iv) The computer simulations show that the image intensity of the Si-rich (002) lattice plane is slightly higher in comparison to that in model 1. The intensity differences depend on the defocus and are within about 10%. A clear distinction between these interface structures can therefore only be successful at a precise microscope and specimen alignment.

IV. EXPERIMENTAL RESULTS

Figure 4 shows a ⟨110⟩ cross-sectional view of a buried $CoSi_2$ layer. The upper and lower interfaces as well as dislocations in the adjacent Si substrate are visible. The average layer thicknesses are about 40 and 80 nm for Co^+ implantations with an energy of 100 and 200 keV, respectively. In many cases these layers show relatively smooth lower interfaces, whereas the upper interfaces are roughened by terraces with height differences of up to 10 nm. Analyses of these terraces show that they are very often bound by {111} facet planes. The dislocations in the region below and above the buried silicide layers are a result of the implantation and annealing procedure. Whereas the $CoSi_2$ layer itself is free of defects, misfit dislocations exist at the interfaces.

HRTEM lattice images of interfaces show as the most important result that regions or domains with different atomic interface structures exist for both upper and lower interfaces. At the lower interfaces of the buried $CoSi_2$ layers interface regions with structures related to models 1 and 2 seem to dominate where the Co atoms are six-fold and eight-fold coordinated, respectively. Under appropriate imaging conditions it is possible to differentiate between structure 1 and structure 2 (Fig. 2). In the latter case the interface contains additional Si atoms, and the contrast of the (002) interface plane is increased by about 10% (Sec. III). Based on such comparisons lattice images of regions at the lower interface can be matched perfectly in many cases by the structure of model 1 with a six-fold Co atom coordination [Fig. 2(a)]. Figure 5 shows as an example experimental lattice images for two defocus values together with the corresponding simulated images.

A third kind of interface structure could be found in sample regions where the upper silicide interface was roughened by formation of terraces. Occasionally this in-

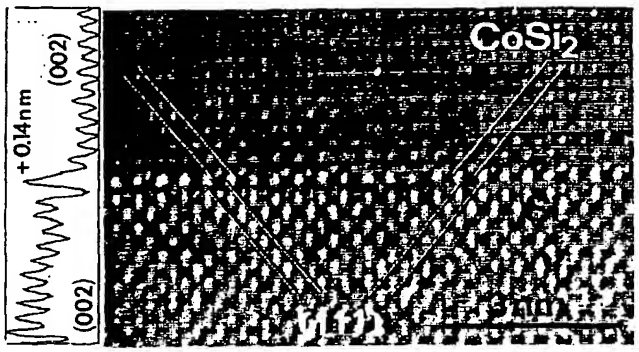

FIG. 6. HRTEM micrograph of a $CoSi_2$/Si(001) Co-rich interface region (model 3, configuration II) in ⟨110⟩ projection. The intensity profile indicates the additional shift of the (002) plane at the interface in [001] direction of 0.14 nm. The shift of the {111} planes is also indicated.

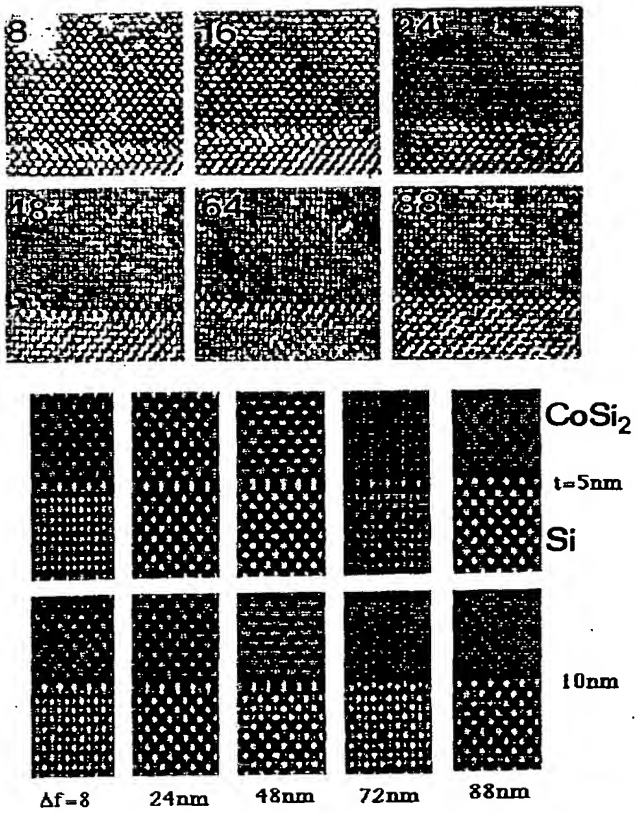

FIG. 7. Comparison between an experimental (upper part) and a simulated (lower part) defocus series of an interface structure of model 3, configuration I (orientation [110]). The defocus values f are given in nm (insets); the specimen thickness is estimated to lie between 5 and 8 nm.

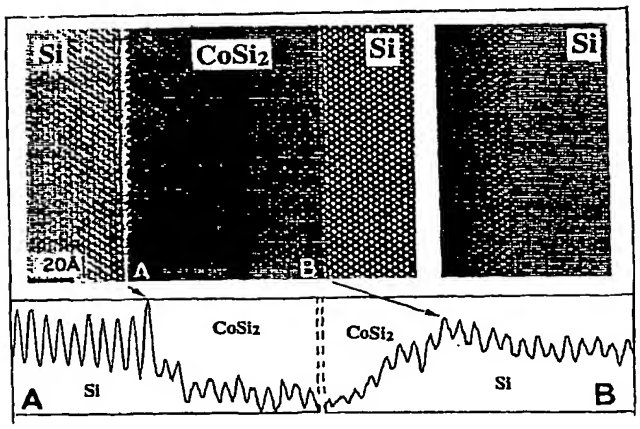

FIG. 8. Different types of crystallographic transitions between the Si matrix and the silicide: atomically sharp transition at the lower interface (left, A); continuous transition, which was often observed at the upper interface (right, B) for two different defocus values. The intensity profiles (below) indicates a transition within about five (002) planes for the latter case.

terface structure was also observed at steps in the lower interface to the bulk. Figure 6 shows the typical HRTEM image contrast at an underfocus of about 32 nm in ⟨110⟩ projection with an additional chain of brighter spots being characteristic of interface images taken under such conditions. Computer simulations based on structure model 3 were performed in order to explain the image contrast of this interface. Furthermore, for these interfaces a {002} lattice plane distance of 0.34 nm (configuration I) or 0.41 nm ($d_{002}+0.14$ nm, configuration II) and displacements of the crossing {111} planes of ± 0.1 nm have been measured which are in good agreement with the corresponding expected values for the proposed interface structure 3 (Sec. III). Figure 7 shows as example a section of a computer-controlled through-focus series of an interface region and a series of simulated images using structure model 3, configuration I. From this comparison it can be concluded that this interface represents the Co-rich interface (structure model 3) where the Co interface atoms are four-fold and six-fold coordinated.

Figure 8 shows an example of an interface region with a continuous transition from the Si lattice to the silicide lattice. The image depicts on the left side the lower interface with a sharp transition, visible also in the profile plot of the {002} planes. The images on the right side show the upper interface for two different defocus values. The corresponding profile plot shows clearly that a continuous transition region exists of a width of about 5 (002) planes.

In addition to the interface images described above we found indications in HRTEM images for interface contrast compatible with a (2×1) reconstruction (not shown) as has been discussed in the literature.[11,13] We observed such a structure mainly in smooth extended silicide interface regions.

As demonstrated above, HRTEM investigations of interfaces on an atomic scale show as the most important novel result regions or domains with different atomic interface structures for both interfaces. Analyses of the abundance of the different interface structures at the upper and lower interfaces of the buried layers show the following trends:

(i) Type 1 interface regions with six-fold coordinated Co interface atoms are most frequently observed and dominate at the lower interfaces.

(ii) Si-rich interface regions (model 2) with eight-fold coordinated Co interface atoms are observed less frequently and predominantly at the lower interfaces.

(iii) Interfaces whose HRTEM images can be related to a Co-rich type (model 3) with four- and six-fold coordinated Co interface atoms are frequently observed near steps and terraces at both interfaces but predominantly at the upper interfaces.

(iv) Interface regions with continuous transitions between the silicide layer and Si were only observed at the upper interface.

The following types of interface dislocations could be identified: (i) misfit dislocations of the Lomer type ($b=a/2\langle110\rangle$), which do not change the coordination of the Co interface atoms in adjacent regions, and (ii) small disloca-

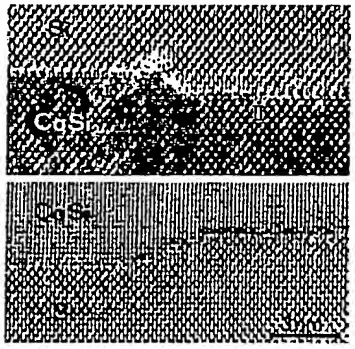

FIG. 9. Steps and facets at the interface (a) Step at the upper interface in ⟨110⟩ projection. The step is 0.8 nm high and shows a {111} facet associated with an orientation change from configuration I to configuration II. (b) Small step at the lower interface (structure model 1) extending over a height of six (002) planes. This step is not associated with a change of the configuration.

tions with a Burgers vector of $b=a/4\langle 111\rangle$. The latter type of dislocation is connected with a change of coordination of the Co atoms. The role of these dislocations for the strain relaxation of the $CoSi_2$ layer has been discussed earlier.[12] Typical of the silicide interfaces observed in this study are also small steps with heights of several (002) plane distances (Fig. 9). Interface planes adjacent to the step often represent different orientation variants corresponding to configurations I and II, respectively [Fig. 9(a)]. This configuration change is associated with an effective local expansion of the Si lattice along the interface by a Burgers vector $b=a/4\langle 111\rangle$ and, therefore, contributes to the misfit accommodation between Si and the silicide layer. Terraces with interface faceting on {111} planes are observed especially for silicide layers which were formed during annealing at longer times.

From electrical characterizations using *I-V*, *I-T*, and *C-V* measurements different average Schottky barrier heights ϕ_{Bn} are obtained for the $CoSi_2/n$-Si(001) top and bottom diodes. Figure 10(a) shows typical results of *I-V* measurements for diodes with two different diode areas. The top diodes show excellent ideality factors, $n=1.03$, and a good area dependence whereas the bottom diodes exhibit worse values, and the forward current does not scale exactly with the diode area. This may be attributed to the end-of-range damage in the Si below the silicide layers, to the higher barrier height of the bottom diodes, or to inhomogeneities of the Schottky barriers (Sec. V). From experiments with Pt/Si diodes (Sec. II) and from the results of the top diodes the dominance of edge currents in *I-V* characteristics of the bottom diodes can be excluded. The comparison between *I-V* and area-independent *I-T* measurements shows the same value for the SBH (within the accuracy of the measurement). The details of the *I-T* and *C-V* measurements are given in a separate paper.[18] The current-voltage curves if plotted semilogarithmically show nonlinear sections in forward directions especially for bottom diodes, in agreement with simulations of the electron transport of nonhomogeneous Schottky barriers.[26] Never-

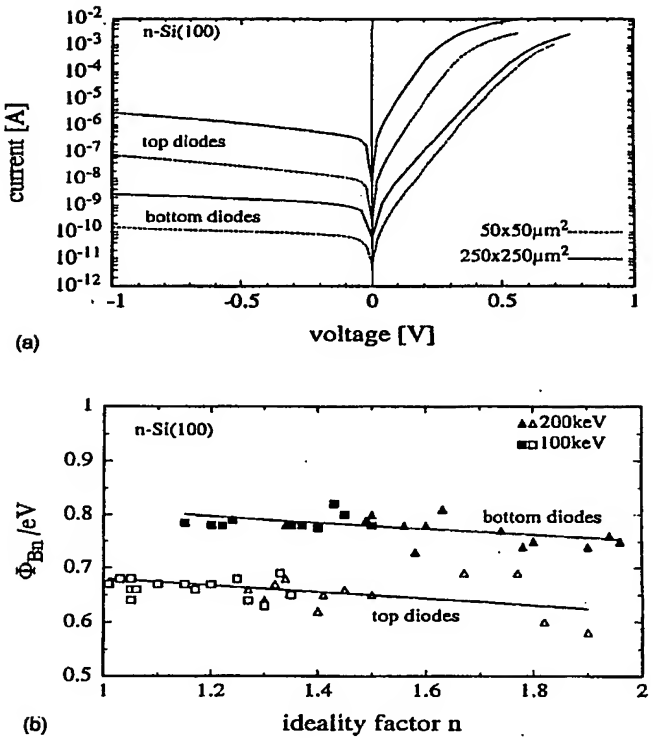

FIG. 10. (a) $I(V)$ characteristics of two typical top and bottom diodes fabricated by 100 keV implantations and measured for two different diode areas; average ideality factors for top diodes: $n=1.03$, for bottom diodes: $n=1.35$ (– –) and $n=1.4$ (—). (b) Average Schottky barrier heights vs ideality factor n for various samples and implantation energies indicated.

theless, there exists a clear difference in the SBH of approximately 0.11 eV between the top and bottom diodes, independently on the diode quality as given by the ideality factor [Fig. 10(b)]. The average SBH is nearly independent on ideality factor, implantation energy, and dose. For the top interface a value of 0.67 ±0.03 eV was observed, for the bottom interface a value of 0.78 ±0.03 eV, respectively.

V. DISCUSSION

The formation of buried cobalt disilicide layers in (001)Si and (111)Si substrates during thermal annealing is the result of a coarsening of the precipitate arrangements formed initially during implantation.[2,3,27–29] Associated with this coarsening process is a considerable redistribution of implanted Co in precipitates within the implanted region.[27–29] Prolonged anneals at high temperatures ($T>1100$ °C) for (001) Si may lead to a breakup of the interconnected $CoSi_2$ layer and formation of a $CoSi_2$ structure with predominantly {111} interfaces.[30] We can assume therefore that the layers investigated represent intermediate stable layer configurations which are transformed by diffusional processes at the higher annealing temperatures of ≤ 1150 °C. This transformation leads to smoothed (001) interfaces or, at the later stages, to roughening possibly resulting in a breakup of the layers.[30] The observed

types of interface structures can be considered as different stages of this dynamic process. The formation of predominantly {001} interfaces for annealed layers must be governed by diffusional processes in the matrix or along interfaces during rapid thermal annealing.

The lower {001} interface is very smooth, with only a few steps. The interface structures of model 1 (Fig. 5) where Co atoms are six-fold coordinated are found to be typical of this interface. This type of interface structure was also reported recently for buried $CoSi_2$ layers formed by ion beam synthesis.[12] Two variants of interface domains exist referred to as configurations I and II, respectively.

The presence of interface regions with the structure of model 2 where Co atoms are eight-fold coordinated was also found although less frequently. Recent structural energy calculations, although for $CoSi_2$/Si(111) interfaces, showed that eight-fold coordination of Co atoms leads to a low-energy interface.[8,31] Such an interface is characterized by an additional layer of Si interface atoms which might be generated by a kick-out mechanism of regular atoms in the adjacent Si as the result of the topotaxial reaction [Fig. 1(b)]. As a variant we found at smooth {001} interface sections indications for a structure compatible with a (2×1) interface reconstruction of Si atoms (Sec. IV).

The upper interfaces show additionally interface regions which can be interpreted by the Co-rich interface structure related to model 3 (Figs. 6 and 7). This interface structure is frequently observed near terraces. Co atoms are four-fold and six-fold coordinated in this model (Sec. III). Our observations of this atomic interface configuration indicate that interface regions with locally higher Co concentrations form in connection with the diffusion of Co along the silicide-silicon interfaces during annealing. From studies of the formation of thin $CoSi_2$ films it has been concluded that the metal atoms constitute the more mobile species during the diffusion and that formation of $CoSi_2$ occurs mostly through the motion of metal atoms.[32–34] The formation of continuous $CoSi_2$ layers with {001} interfaces during the later stages of annealing seems to be connected with preferential diffusion of Co along the interfaces. The atomic arrangement of Co-rich interface regions, for which the structure model 3 is proposed [Fig. 1(c)], is therefore presumably metastable, and the existence of other forms is likely.

A unique feature of the upper interface is the presence of regions with continous transitions, as opposed to an atomically abrupt lower interface (Fig. 8). Although the atomic structure of this continuous interface is not clear yet it seems unlikely that steps at the interface running perpendicular to the viewing direction are responsible for the observed asymmetry in the lattice images since steps are present at both interfaces as can be seen in Fig. 9. This asymmetry in the occurrence of such interfaces with continuous transitions may reflect differences in the dynamical processes leading to changes of the interface morphology during rapid thermal annealing.

The silicides $CoSi_2$ and $NiSi_2$ are unique in that they form epitaxial Schottky barrier interfaces of atomically high perfection with Si.[20,35] For $CoSi_2$/Si(001) diodes

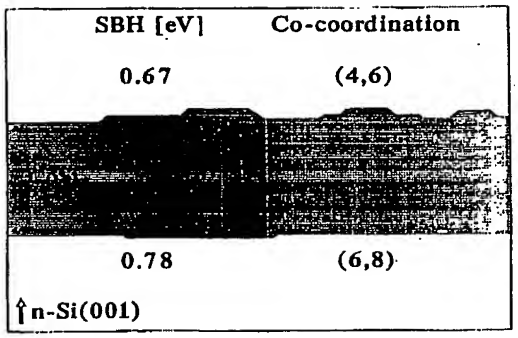

FIG. 11. Correlation of interface structure with SBH values for ion-implanted $CoSi_2$/n-Si(001) layers (schematic), with {111} facets and dominant atomic interface structure, as given by (n)-fold Co interface atom coordination.

which were fabricated under experimental conditions identical with those used in the fabrication of the $CoSi_2$ layers investigated by HRTEM clear differences are measured for the Schottky barrier heights of the top and bottom interfaces, respectively (Sec. IV). The differences in type and local distribution of the atomic interface structures of the lower and the upper metal-semiconductor interfaces of the buried silicide layers are suggestive of a correlation with this result. The observations relevant for such a correlation concern the following differences:

(i) the different atomic interface structures: the Co-rich interface (model 3) is found predominantly at the upper interfaces for which a smaller SBH of 0.67 eV was measured. Similarly, interfaces with continuous transitions are present only at the upper interface. Interface structures with six-fold and eight-fold coordination of Co interface atoms, respectively, are predominantly found at the lower interfaces for which the larger SBH of 0.78 eV was measured;

(ii) the small but different fraction of {111} interface structure at facets and steps;

(iii) the interface defects, such as dislocations and their associated strain effects. Such defects are expected to have only a limited influence on the SBH.

Differences in Schottky barrier heights have also been observed recently for $NiSi_2$/Si(111) interfaces of A- and B-type orientation and attributed to differences of the atomic interface structures.[14,36] Based on defect density measurements at such interfaces, defects were ruled out as a possible reason for the different Schottky barrier heights.[36] In a recent theoretical study for $NiSi_2$, the difference was attributed to a different charge transfer between the $NiSi_2$ layer and the Si substrate.[37] The charge transfer between metal and semiconductor across the interface may be modeled by the difference between the metal and semiconductor electronegativities.[38] The Schottky barrier height is determined by the electric dipole moment normal to the interface, i.e., by the charge transfer and the distance normal to the interface over which this transfer takes place. This distance will depend upon the geometrical arrangement of interface atoms, i.e., the coor-

dination of Co interface atoms, and therefore upon the type and distribution of interface structures which are found to be different in our case for the upper and the lower interfaces. On the other hand, the presence of a higher areal density of steps and {111} facets and of regions with a continuous transition at the upper $CoSi_2$/Si(001) interfaces should also be relevant for the observed lower values of the Schottky barriers. Figure 11 shows a schematic representation of the structure of the upper and lower $CoSi_2$/Si(001) interface together with the dominant Co interface atom coordinations and the average Schottky barrier heights measured for *n*-Si substrates. Our results suggest a correlation of smaller SBH values with smaller Co interface atom coordination with possible contributions from {111} facets. This conclusion is therefore in support of the idea[39–41] that the current transport across the metal-semiconductor interface is determined by locally different Schottky barriers.

VI. CONCLUSIONS

Structural investigations by quantitative high-resolution transmission electron microscopy and electrical measurements of Schottky barrier heights have been performed on interfaces of buried implanted $CoSi_2$ layers in (001) oriented Si substrates and have led to the following results:

(i) Under the conditions of implantation and rapid thermal annealing treatment applied the buried $CoSi_2$/Si(001) layers are characterized by excellent epitaxial growth and relatively smooth {001} interfaces. The upper interfaces are more roughened and are often bound by {111} facet planes.

(ii) Three different types of atomic {001} interface structures were observed (Fig. 1): six-fold coordination of the Co interface atoms, eight-fold Co coordination representing a Si-rich interface, and Co-rich interfaces for which the Co interface atoms can be six-fold and four-fold coordinated and for which the structure model 3 is proposed. Co-rich interfaces are found predominantly in regions near steps and facets and are more frequently observed at the upper interfaces. Our proposal of a novel Co-rich interface structure is consistent with considerations about the formation process of the buried layers.

(iii) The observations of Co-rich interface regions preferentially near steps and {111} facets indicate that Co diffusion takes place along the interfaces eventually leading to energetically metastable interface configurations. As shown by earlier studies (Sec. IV) both the formation process resulting from precipitate coarsening, as well as the decomposition of interconnected continuous buried $CoSi_2$ layers, are associated with a considerable redistribution of Co within the implanted regions. Therefore one has to expect also that different interface structures on an atomic scale, resulting from the dynamic changes in layer morphology during annealing, can be observed at room temperature, i.e., when the Co redistribution during layer formation has ceased. Our results confirm this view.

(iv) The asymmetry between the atomic interface structures observed at the lower and the upper interfaces is the likely origin for differences in the Schottky barrier heights measured for top and bottom $CoSi_2$/Si (001) Schottky diodes (Figs. 10 and 11).

ACKNOWLEDGMENTS

We would like to thank R. Jebasinski and M. Gebauer for the implantations and Ch. Dieker for the expert preparation of the cross-section specimens. We acknowledge helpful discussions with R. Jebasinski, Professor H. Lüth, Dr. S. Mantl, and Professor K. Urban. One of the authors (W.J.) is grateful for stimulating discussions with Dr. P. Stadelmann.

[1] A. E. White, K. T. Short, R. C. Dynes, J. P. Garno, and J. M. Gibson, Mater. Res. Soc. Symp. Proc. 74, 481 (1987); Appl. Phys. Lett. 50, 9 (1987).
[2] A. E. White, K. T. Short, R. C. Dynes, J. M. Gibson, and R. Hull, Mater. Res. Soc. Symp. Proc. 107, 3 (1988).
[3] K. Kohlhof, S. Mantl, B. Stritzker, and W. Jäger, Nucl. Instrum. Methods Phys. Res. B 39, 276 (1989).
[4] A. H. Van Ommen, J. J. M. Ottenheim, and C. W. T. Bulle-Lieuwma, Appl. Surf. Sci. 38, 197 (1989).
[5] J. C. Hensel, A. F. J. Levi, R. T. Tung, and J. M. Gibson, Ultramicroscopy 14, 1 (1984).
[6] A. Schüppen, S. Mantl, L. Vescan, S. Woiwod, R. Jebasinski, and H. Lüth, Mater. Sci. Eng. B 12, 157 (1992).
[7] S. P. Murarka, "Properties and Applications of Silicides," in *Microelectronic Materials and Processes*, edited by R. A. Levy (Academic, Kluwer, 1989), p. 275.
[8] D. R. Hamann, Phys. Rev. Lett. 60, 313 (1988).
[9] D. Cherns, C. J. D. Hetherington, and C. J. Humphreys, Philos. Mag. A 49, 165 (1984).
[10] R. Hull, Y. F. Hsieh, K. T. Short, A. E. White, and D. Cherns, Mater. Res. Soc. Symp. Proc. 183, 91 (1990).
[11] D. Loretto, J. M. Gibson, and S. M. Yalisove, Phys. Rev. Lett. 63, 298 (1989); Thin Solid Films 184, 309 (1990).
[12] C. W. T. Bulle-Lieuwma, A. F. DeJong, and D. E. W. Vandenhoudt, Philos. Mag. A 64, 255 (1991).
[13] S. J. Pennycook, D. E. Jesson, and M. F. Chisholm, Inst. Phys. Conf. Ser. No. 100, 51 (1989).
[14] R. T. Tung, A. F. J. Levi, J. P. Sullivan, and F. Schrey, Phys. Rev. Lett. 66, 72 (1991).
[15] R. T. Tung, A. F. J. Levi, and J. M. Gibson, J. Vac. Sci. Technol. B 4, 1435 (1986); Phys. Rev. B 33, 7077 (1986).
[16] R. Jebasinski, S. Mantl, Ch. Dieker, and W. Jäger, Nucl. Instrum. Methods Phys. Res. B 64, 99 (1992).
[17] A. Schüppen, S. Mantl, L. Vescan, and H. Lüth, in *Proceedings of the 20th ESSDERC*, edited by W. Eccleston and P. J. Rossen (Hilger, Bristol 1990), p. 45.
[18] A. Schüppen, Berichte des Forschungszentrums Jülich, Report No. 2746, 1993.
[19] P. Stadelmann, Ultramicroscopy 21, 131 (1987).
[20] D. Cherns, G. R. Anstis, J. L. Hutchison, and J. C. H. Spence, Philos. Mag. A 46, 849 (1982).
[21] R. T. Tung and J. M. Gibson, J. Vac. Sci. Technol. A 3, 987 (1985).
[22] P. Werner, R. Mattheis, D. Hesse, R. Hillebrand, and J. Heydenreich, Phys. Status. Solidi A 116, 81 (1989).
[23] C. W. T. Bulle-Lieuwma, A. F. De Jong, A. H. Van Ommen, J. F. Van der Veen, and J. Vrijmoeth, Appl. Phys. Lett. 55, 648 (1989).
[24] A. Catana, P. Lu, and D. J. Smith, Mater. Res. Soc. Symp. Proc. 183, 105 (1990).
[25] A. Catana, P. E. Schmid, S. Rieubland, F. Levy, and P. Stadelmann, J. Phys. Condens. Matter 1, 3999 (1989).
[26] J. P. Sullivan, R. T. Tung, M. R. Pinto, and W. R. Graham, J. Appl. Phys. 70, 1 (1991).
[27] C. W. T. Bulle-Lieuwma, A. H. van Ommen, and L. J. van Ijzendoorn, Appl. Phys. Lett. 54, 244 (1989).
[28] K. Kohlhof, S. Mantl, B. Stritzker, and W. Jäger, Appl. Surf. Sci. 38, 207 (1989).

[29] P. F. P. Fichtner, W. Jäger, K. Rademacher, and S. Mantl Nucl. Instrum. Methods Phys. Res. B 59/60, 632 (1991).
[30] M. F. Wu, A. Vantomme, H. Pattyn, G. Langouche, K. Maex, J. Vanhellemont, J. Vanacken, H. Vloeberghs, and Y. Bruynseraede, Nucl. Instrum. Methods Phys. Res. B 45, 658 (1990).
[31] P. J. Van den Hoek, W. Ravenek, and E. J. Baerends, Phys. Rev. Lett. 60, 1743 (1988).
[32] F. M. D'Heurle and C. S. Petersson, Thin Solid Films 128, 283 (1985).
[33] F. M. D'Heurle and P. Gas, J. Mater. Res. 1, 205 (1986).
[34] O. Thomas, P. Gas, A. Chari, F. K. LeGouches, A. Michel, G. Scilla, and F. M. D'Heurle, J. Appl. Phys. 64, 2973 (1988).
[35] J. M. Gibson, J. C. Bean, J. M. Poate, and R. T. Tung, Appl. Phys. Lett. 41, 818 (1982).
[36] J. Vrijmoeth, J. F. Van der Veen, D. R. Heslinga, and T. M. Klapwijk, Phys. Rev. B 42, 9598 (1990).
[37] G. P. Das, P. Blöchl, O. K. Andersen, N. E. Christensen, and O. Gunnarsson, Phys. Rev. Lett. 63, 1168 (1989).
[38] W. Mönch, Rep. Prog. Phys. 53, 221 (1990).
[39] R. T. Tung, Appl. Phys. Lett. 58, 2821 (1991).
[40] J. H. Werner and H. H. Güttler, Phys. Scrip. T 39, 258 (1991).
[41] J. M. Vandenberg, A. E. White, R. Hull, K. T. Short, and S. M. Yalisove, J. Appl. Phys. 67, 787 (1990).